

# Backbone exponent and annulus crossing probability for planar percolation

Pierre Nolin,<sup>1,\*</sup> Wei Qian,<sup>2,†</sup> Xin Sun,<sup>3,‡</sup> and Zijie Zhuang<sup>4,§</sup>

<sup>1</sup>*City University of Hong Kong*

<sup>2</sup>*City University of Hong Kong (on leave from CNRS, Laboratoire de Mathématiques d'Orsay)*

<sup>3</sup>*Beijing International Center for Mathematical Research, Peking University*

<sup>4</sup>*Wharton Statistics and Data Science Department, University of Pennsylvania*

We report the recent derivation of the backbone exponent for 2D percolation. In contrast to previously known exactly solved percolation exponents, the backbone exponent is a transcendental number, which is a root of an elementary equation. We also report an exact formula for the probability that there are two disjoint paths of the same color crossing an annulus. The backbone exponent captures the leading asymptotic, while the other roots of the elementary equation capture the asymptotic of the remaining terms. This suggests that the backbone exponent is part of a conformal field theory (CFT) whose bulk spectrum contains this set of roots. Our approach is based on the coupling between SLE curves and Liouville quantum gravity (LQG), and the integrability of Liouville CFT that governs the LQG surfaces.

*Introduction.*—The fractal geometry of critical percolation clusters [1] is a classical topic in statistical physics. For two-dimensional Bernoulli percolation, the exact values of many fractal dimensions are explicitly known. These values were often first discovered in physics and later proved using probabilistic methods. For instance, the dimensions of the percolation cluster, cluster boundary, and pivotal points are  $\frac{91}{48}$ ,  $\frac{7}{4}$ , and  $\frac{3}{4}$ , respectively. Despite these successful examples, the fractal dimension of the backbone of a percolation cluster remained elusive for a long time. The backbone is the remaining part of a percolation cluster after removing the dangling ends, where electrical current between distant vertices would flow. In this Letter, we report recent progress on the exact derivation of the backbone exponent and the related annulus crossing probability.

The backbone dimension  $D_B$  can be characterized as follows. Consider critical Bernoulli percolation on a triangular lattice of small mesh size, where each site is colored black or white with equal probability. Let  $A(r, R)$  be the annulus of inner radius  $r$  and outer radius  $R$ . As the mesh size tends to 0, the probability that there are two disjoint black paths crossing an annulus  $A(r, R)$  converges to a limiting probability  $p_B(r, R)$ . There exists an exponent  $x_B$  such that  $p_B(r, R)$  decays as  $(\frac{r}{R})^{x_B + o(1)}$  as  $r/R \rightarrow 0$  [2]. Then we have  $D_B = 2 - x_B$ . The exponent  $x_B$  is known as the backbone exponent, or the monochromatic two-arm exponent.

In general, arm exponents of percolation describe the asymptotic behavior of the annulus crossing probability. The monochromatic  $k$ -arm exponent corresponds to  $k$  disjoint black paths. For  $k \geq 2$ , the polychromatic  $k$ -arm exponents correspond to  $k$  disjoint paths, not all of which are of the same color. The one-arm exponent and the polychromatic  $k$ -arm exponents are explicitly known to be  $\frac{5}{48}$  and  $\frac{k^2-1}{12}$ , respectively [3, 4]. These in particular give the dimensions  $\frac{91}{48}$ ,  $\frac{7}{4}$ , and  $\frac{3}{4}$  mentioned above.

In our recent work [5], the exact value of  $x_B$  is shown

to be the unique solution in  $(\frac{1}{4}, \frac{2}{3})$  to

$$\frac{\sqrt{36x+3}}{4} + \sin\left(\frac{2\pi\sqrt{12x+1}}{3}\right) = 0. \quad (1)$$

The numerical value is 0.3566668..., which matches well with numerical simulations in [6]. Using this expression, we show that  $x_B$  is a transcendental number, which is surprising since all other known exponents in Bernoulli percolation are rational.

Our derivation is based on the convergence of 2D percolation towards Schramm-Loewner evolution (SLE) [7] with parameter 6. We focus on site percolation on the triangular lattice because the convergence to  $\text{SLE}_6$  is established only for this lattice [8]. This convergence is believed to hold for a broad class of 2D Bernoulli percolation, such as bond percolation on the square lattice. Another key ingredient in our derivation is the coupling between SLE and Liouville quantum gravity (LQG), which describes the scaling limit of statistical physics models on random triangulations. The quantum gravity method for deriving fractal dimension has for example been applied to the dimension  $4/3$  of the Brownian frontier [9]. This idea, known as the KPZ relation [10], was put into a mathematical framework in [11].

Compared to [9], the main novelty of our approach is to incorporate the integrability of Liouville conformal field theory, the field theory that governs the random surfaces in LQG [12], into the study of SLE. This approach was developed in [13] and has been successfully used in several problems. In fact, we use this method to derive in [14] that  $p_B(r, R)$  exactly equals

$$\frac{q^{-\frac{1}{12}}}{\prod_{n=1}^{\infty} (1 - q^{2n})} \sum_{s \in \mathcal{S}} \frac{-\sqrt{3} \sin(\frac{2\pi}{3}\sqrt{3s}) \sin(\pi\sqrt{3s})}{\cos(\frac{4\pi}{3}\sqrt{3s}) + \frac{3\sqrt{3}}{8\pi}} q^s, \quad (2)$$

where  $\mathcal{S} = \{s \in \mathbb{C} : \sin(4\pi\sqrt{\frac{s}{3}}) + \frac{3}{2}\sqrt{s} = 0\} \setminus \{0, \frac{1}{3}\}$  and  $q = r/R$ . The numerical values for  $\mathcal{S}$  are  $\{0.440, 2.194 \pm 0.601i, 5.522 \pm 1.269i, \dots\}$ . This equation is related to (1)

by  $s = x + \frac{1}{12}$ . Hence (2) provides a physical interpretation of roots in (1).

The analogous annulus crossing probabilities for the one-arm exponent and the alternating  $2k$ -arm exponents were derived by Cardy [15], and can be expressed in a similar form as (2), except that all the exponents and coefficients in the expansion are rational. Our derivation of (2) is based on a method developed in [16]. The same method also recovers Cardy's result for the one-arm case and the alternating two-arm case. In this Letter we present the key ideas in deriving  $x_B$  and  $p_B(r, R)$ .

*Conformal radii of SLE and percolation exponents.*— The first step in our derivation of (1) is to encode the backbone exponent using the conformal radius of a domain bounded by an  $\text{SLE}_6$  curve. This type of encoding can be done for various percolation exponents. We first demonstrate this using the example of the one-arm exponent  $x_1$ . On the triangular lattice with small mesh size, consider Bernoulli site percolation in an approximation of the unit disk, as shown in Figure 1, where each site is represented by a hexagon. We set the boundary to be all black, namely, the hexagons not drawn in Figure 1 are black. Then as the mesh size tends to zero, the interfaces separating the black and white clusters converge to a collection of loops, which together form the so-called conformal loop ensemble with parameter  $\kappa = 6$  ( $\text{CLE}_6$ ) on the disk [17]. Each loop in  $\text{CLE}_6$  locally looks like the  $\text{SLE}_6$  curve introduced by Schramm [7], which is not self-crossing but has self intersections.

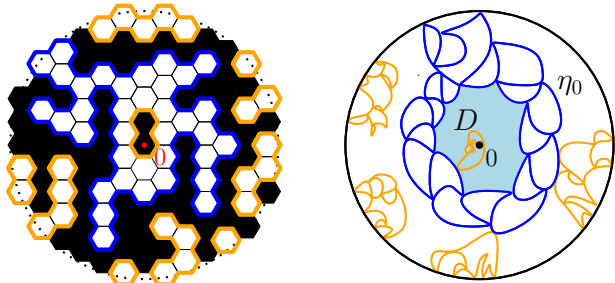


FIG. 1. **Left:** Bernoulli percolation on a triangular lattice on the unit disk. The blue loop is the outermost percolation interface surrounding the origin, whose scaling limit is  $\eta_0$  on the right. **Right:**  $\text{CLE}_6$  on the unit disk. The loops are nested, non-simple, and may touch each other and the boundary.

Let  $\eta_0$  be the outermost loop in  $\text{CLE}_6$  that surrounds the origin. Let  $D$  be the complementary connected component of  $\eta_0$  containing the origin, as shown in Figure 1 (right). Let  $f$  be a conformal map from the unit disk to  $D$  such that  $f(0) = 0$ . The conformal radius  $\text{CR}(0, D)$  of  $D$  viewed from the origin  $0 \in \mathbb{C}$  is defined as  $|f'(0)|$ . Let  $p(r, 1)$  be the probability that there exists a black crossing of  $A(r, 1)$ , which is equivalent to the distance from 0 to the outermost percolation interface being less than  $r$ . By the Koebe 1/4 theorem, the ratio between  $\text{CR}(0, D)$  and the distance from 0 to  $\eta_0$  is between 1 and 4. The one-arm exponent  $x_1$  is therefore given by

$p(r, 1) \approx \mathbb{P}[\text{CR}(0, D) \leq r] = r^{x_1+o(1)}$  as  $r \rightarrow 0$ . Hence,

$$x_1 = \inf\{x \in \mathbb{R} : \langle \text{CR}(0, D)^{-x} \rangle = \infty\}. \quad (3)$$

The value  $x_1 = 5/48$  was originally established in [4] by estimating  $\mathbb{P}[\text{CR}(0, D) \leq r]$ . The exact formula  $\langle \text{CR}(0, D)^{-x} \rangle = \frac{1}{2 \cos(\frac{\pi}{3} \sqrt{12x+1})}$  was further obtained in [18], from which one can also extract  $x_1$ .

The backbone exponent  $x_B$  can be encoded using a similar idea. For each loop in a  $\text{CLE}_6$  on the unit disk, its outer boundary is defined to be the boundary of the unbounded component after removing the loop from the plane. Then the outer boundaries of all the  $\text{CLE}_6$  loops form a random collection of simple loops, each of which looks like an  $\text{SLE}_\kappa$  curve with  $\kappa = \frac{8}{3}$  [19]. Let  $D_b$  be the domain bounded by the outermost loop surrounding the origin in this loop ensemble. Then

$$x_B = \inf\{x \in \mathbb{R} : \langle \text{CR}(0, D_b)^{-x} \rangle = \infty\}. \quad (4)$$

To see (4), consider the *filled percolation interfaces* obtained by filling the fjords of percolation interfaces (see the blue loop in Figure 2 (left)). If the distance from 0 to the outermost filled percolation interface is less than  $r$ , then we need to flip at least two black points to disconnect all black crossings in  $A(r, 1)$ . By the max-flow min-cut theorem, there exist two disjoint black crossings in  $A(r, 1)$ . In fact, the probabilities of these two events share the same exponent as  $r \rightarrow 0$ . Moreover, these filled percolation interfaces converge to outer boundaries of the  $\text{CLE}_6$  loops. This gives (4) similar to (3).

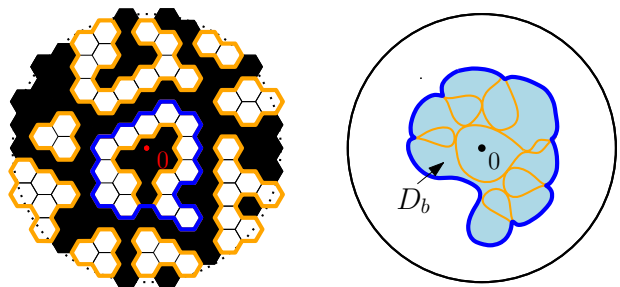


FIG. 2. **Left:** Percolation interfaces are colored orange. The blue loop is an example of a filled interface, which encloses all black points that can be surrounded by a white cluster together with an additional black point. It is the outermost one surrounding the origin. **Right:** Filled percolation interfaces converge to the outer boundaries of  $\text{CLE}_6$  loops. The blue loop is the outermost one surrounding 0, and  $D_b$  is the domain enclosed by this blue loop.

Now the value of  $x_B$  specified by (4) follows from the exact formula of  $\langle \text{CR}(0, D_b)^{-x} \rangle$ , which is

$$\frac{3\sqrt{3}}{4} \sin\left(\frac{\pi}{2} \sqrt{12x+1}\right) \left( \frac{\sqrt{36x+3}}{4} + \sin\left(\frac{2\pi\sqrt{12x+1}}{3}\right) \right)^{-1}. \quad (5)$$

Below we explain how  $\langle \text{CR}(0, D_b)^{-x} \rangle$  and  $p_B(r, R)$  arise in the 2D quantum gravity framework.

*The quantum gravity approach.*— Consider Bernoulli site percolation on a random triangulation. We can view the random triangulation as a discrete model for 2D quantum gravity [20], and percolation as a conformal matter with central charge  $c_M = 0$ . Assume the random triangulation has the disk topology. Then in the continuum limit, the 2D quantum gravity can be described by the Liouville field theory on the disk with central charge  $c_L = 26 - c_M = 26$ . The action of the theory is

$$S_L[\phi] = \int_{\mathbb{U}} \left( \frac{1}{4\pi} |\nabla\phi|^2 + \mu e^{\gamma\phi} \right) d^2x + \int_{\partial\mathbb{U}} \left( \frac{Q\phi}{2\pi} + \nu e^{\frac{\gamma}{2}\phi} \right) dl. \quad (6)$$

The background charge  $Q > 2$  is related to  $c_L$  by  $c_L = 1 + 6Q^2$ , hence  $Q = \sqrt{25/6}$ . We take  $\mathbb{U}$  to be the flat unit disk  $\{|z| \leq 1\}$  so that the charge is supported on the boundary. The coupling constant  $\gamma \in (0, 2)$  is related to  $Q$  by  $Q = \frac{\gamma}{2} + \frac{2}{\gamma}$ , hence  $\gamma = \sqrt{8/3}$ . The bulk cosmological constant  $\mu$  and the boundary cosmological constant  $\nu$  are allowed to vary. Consider the field  $\phi$  whose distribution is given by  $e^{\frac{\gamma}{2}\phi(1)} \cdot e^{\gamma\phi(0)} \cdot e^{-S_L[\phi]} D\phi$ . The continuum limit of percolation on a random triangulation of the disk can be described by  $\text{CLE}_6$  on  $\mathbb{U}$  with a random geometric background: the area measure is  $e^{\gamma\phi} d^2x$  on  $\mathbb{U}$ , and the boundary length measure is  $e^{\frac{\gamma}{2}\phi} dl$  on  $\partial\mathbb{U}$ . Here  $0 \in \mathbb{U}$  and  $1 \in \partial\mathbb{U}$  correspond to one bulk point and one boundary point on the triangulation, which are marked to specify how the random surface is conformally parameterized by  $\mathbb{U}$ . A version of this is rigorously proved in [21].

From now on we set  $\mu = 0$  in  $S_L[\phi]$  and write it as  $S_L^\nu[\phi]$ , only allowing  $\nu$  to vary. Then

$$\int_{\phi: \mathbb{U} \rightarrow \mathbb{R}} F \left( \int_{\partial\mathbb{U}} e^{\frac{\gamma}{2}\phi} dl \right) e^{\gamma\phi(0)} e^{-S_L^\nu[\phi]} D\phi \quad (7)$$

is proportional to  $\int_0^\infty F(L) e^{-\nu L} L^{-\frac{3}{2}} dL$  for any test function  $F$ . On the discrete side, consider a polygon of length  $p$ . For each triangulation of it with an interior marked point and  $n$  faces we assign weight  $a^n b^p$ . Then for critical  $a$  and  $b$ , as  $p \rightarrow \infty$  the total weight grows as  $p^{-\frac{3}{2}}$ . From both perspectives, we can say that  $L^{-\frac{3}{2}}$  is the partition function for the random disk in the pure 2D quantum gravity which has boundary length  $L$ , one interior marked point, and no area constraint [22]. We denote such a random disk by  $\text{QD}_1(L)$ . We do not mark any boundary point on  $\text{QD}_1(L)$ , hence the boundary insertion  $e^{\frac{\gamma}{2}\phi(1)}$  does not appear in (7).

Suppose  $\text{QD}_1(L)$  is conformally realized on  $\mathbb{U}$  with the marked point at 0. Consider  $\text{CLE}_6$  on  $\mathbb{U}$  as in Figure 2 with  $D_b$  defined above (4), and let  $\eta$  be the boundary of  $D_b$ . The curve  $\eta$  cuts  $\text{QD}_1(L)$  into two pieces of random surfaces which are independent once conditioned on the length of  $\eta$ . This independence in the triangulation setting is clear; see Figure 3. In the continuum, results of this type were pioneered by [23]. A highly nontrivial conclusion from this approach is that the surface inside  $\eta$  is another copy of  $\text{QD}_1$ . In fact we can write the following

equality of partition functions:

$$\int_0^\infty Z(L, \ell) \times \ell \times \ell^{-\frac{3}{2}} d\ell = L^{-\frac{3}{2}}, \quad (8)$$

where  $Z(L, \ell)$  is the partition function of the random surface bounded by  $\partial\mathbb{U}$  and  $\eta$  with given boundary lengths, and  $\ell^{-\frac{3}{2}}$  is the partition function of  $\text{QD}_1(\ell)$  which describes the random surface inside  $\eta$ . The additional factor  $\ell$  is the length of  $\eta$ , that counts the number of ways in which the two surfaces can be glued together, since we do not mark a point on  $\eta$ .

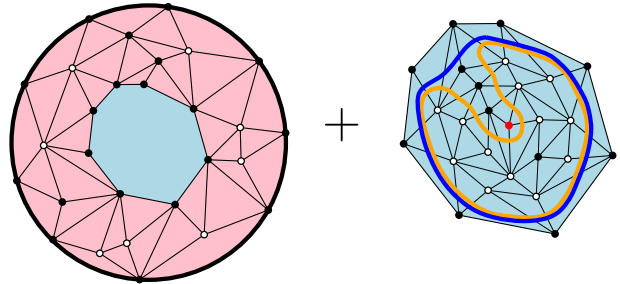


FIG. 3. Bernoulli site percolation on a random triangulation of the disk. The outermost filled percolation interface colored in blue divides the random triangulation into two parts. These two parts are independent conditioned on the number of vertices along the filled interface. In the continuum limit, this corresponds to (8).

We are now ready to explain the key equation

$$\int_0^\infty Z(L, \ell) \times \ell \times \ell^{-\frac{3}{2}+a} d\ell = L^{-\frac{3}{2}+a} \langle \text{CR}(0, D_b)^{x(a)} \rangle, \quad (9)$$

where  $x(a) = -\frac{1}{3}a(a-1)$ . This is a modification of the surface gluing equation (8). The surface bounded by  $\partial\mathbb{U}$  and  $\eta$  stays the same, while the surface corresponding to  $\text{QD}_1(\ell)$  is modified to a new random surface with partition function  $\ell^{-\frac{3}{2}+a}$ . To describe this new surface, we note that if  $e^{\gamma\phi(0)}$  in (7) is replaced by  $e^{\alpha\phi(0)}$ , then (7) becomes proportional to  $\int_0^\infty F(L) e^{-\nu L} L^{\frac{\gamma}{2}(\alpha-\gamma)-\frac{3}{2}} dL$ . This defines a random surface with partition function  $L^{\frac{\gamma}{2}(\alpha-\gamma)-\frac{3}{2}}$  just as how  $\text{QD}_1(L)$  is defined from (7). Taking  $\alpha = \gamma + \frac{\gamma}{2}a$  and  $\gamma = \sqrt{8/3}$ , this defines the random surface in (9) with partition function  $\ell^{-\frac{3}{2}+a}$ .

Once the surface corresponding to  $\text{QD}_1(\ell)$  in (8) is modified, the surface  $\text{QD}_1(L)$  on the right side of (8) changes to a surface with partition function  $L^{-\frac{3}{2}+a}$  via the same mechanism. The additional factor  $\langle \text{CR}(0, D_b)^{x(a)} \rangle$  in (9) arises because when modifying the bulk insertion  $e^{\gamma\phi(0)}$  to  $e^{\alpha\phi(0)}$ , we assumed that both the smaller surface  $\text{QD}_1(\ell)$  and the larger surface  $\text{QD}_1(L)$  are conformally realized on  $\mathbb{U}$ . Therefore, we first need to apply a conformal map  $f$  from  $D_b$  to  $\mathbb{U}$  while fixing 0. This results in a factor of  $|f'(0)|^{x(a)}$  with  $x(a) = 2\Delta_\alpha - 2\Delta_\gamma$ , where  $\Delta_\alpha = \frac{\alpha}{2}(Q - \frac{\alpha}{2})$  is the scaling dimension of the bulk insertion  $e^{\alpha\phi(0)}$  in Liouville theory. By definition,  $|f'(0)|^{-1} = \text{CR}(0, D_b)$ , which gives the right side of (9).

Equations like (9) relate the conformal radii of domains bounded by SLE curves with the partition function of random surfaces in 2D quantum gravity with given lengths. As demonstrated in [13], in certain cases, the partition function of the random surfaces can be exactly solved using the structure constants of boundary Liouville theory [24], hence such relations provide the exact formula for the conformal radii. However, since the surface corresponding to  $Z(L, \ell)$  has a random conformal modulus, the method in [13] does not readily give a formula for  $Z(L, \ell)$ . A key step in [5] to derive (1) is to find an effective variant of  $\text{CR}(0, D_b)$  such that it still encodes the backbone exponent; and moreover, the analog of  $Z(L, \ell)$  is solvable using the method in [13]. The strategy is to consider a chain of adjacent loops connecting the disk boundary to the boundary of  $D_b$ , which forms a sequence of shrinking domains whose conformal radii can be solved step by step. The precise implementation of this strategy involves a Poisson point process of a special variant of  $\text{SLE}_6$  called the  $\text{SLE}_6$  bubble [25]. The detail can be found in [5, Section 2].

The ratio between  $\text{CR}(0, D_b)$  and its effective variant in [5] is another conformal radius that can be solved using the method from [13]. This gives (5), as done in [14]. Now  $Z(L, \ell)$  can be solved from (5) and (9). This is the starting point of the derivation of (2) for  $p_B(r, R)$ .

*Quantum gravity on the annulus.*— Depending on whether  $\eta$  touches  $\partial\mathbb{U}$ , the partition function  $Z(L, \ell)$  of the random surface bounded by  $\eta$  and  $\partial\mathbb{U}$  can be divided into two parts:  $Z^{\text{nt}}(L, \ell)$  and  $Z^{\text{t}}(L, \ell)$ , where  $Z^{\text{nt}}(L, \ell)$  corresponds to when  $\eta$  does not touch  $\partial\mathbb{U}$ . From the triangulation setting in Figure 3, we see that  $Z^{\text{nt}}(L, \ell)$  describes a random annulus in the pure quantum gravity with boundary lengths  $L$  and  $\ell$ , coupled with a percolation configuration for which the monochromatic two-arm crossing occurs. In the Liouville framework, this random annulus can be decomposed into three components: the Liouville field, the conformal matter, and the bosonic ghost field [26]. We conformally parameterize the annulus as the finite cylinder  $\mathcal{C}_\tau$  obtained by identifying  $[0, \tau] \times \{0\}$  with  $[0, \tau] \times \{1\}$  on  $[0, \tau] \times [0, 1]$ . Then the modulus  $\tau$  of the annulus is random and the partition function of a given  $\tau$  is the product of the partition function of three components. In our case, the partition function for the conformal matter is simply  $p_B(e^{-2\pi\tau}, 1)$ . The ghost partition function on  $\mathcal{C}_\tau$  is  $Z_{\text{ghost}}(\tau) = \eta(2i\tau)^2$  [27]. Therefore for test functions  $f, g$  we have  $\int_0^\infty e^{-\nu_1 L} e^{-\nu_2 \ell} f(L)g(\ell)Z^{\text{nt}}(L, \ell)d\ell dL$

$$\propto \int_0^\infty p_B(e^{-2\pi\tau}, 1) \langle f(L_0)g(L_1) \rangle_\tau Z_{\text{ghost}}(\tau) d\tau, \quad (10)$$

where  $\langle f(L_0)g(L_1) \rangle_\tau$  is averaging over the Liouville theory on  $\mathcal{C}_\tau$  with boundary cosmological constants  $\nu_1$  and  $\nu_2$ , and  $L_0$  and  $L_1$  are the two boundary lengths. Similarly to (7), we set the bulk cosmological constant to be 0 since there is no area constraint on the surface.

As done in [16], for  $\nu_1 = \nu_2 = 0$ , solving the Liouville theory on the annulus gives

$$\langle L_0 e^{-L_0} L_1^{ix} \rangle_\tau = \frac{1}{\sqrt{2}\eta(2i\tau)} \cdot e^{-\frac{\pi\gamma^2 x^2 \tau}{4}} \cdot \frac{\pi\gamma x \Gamma(1+ix)}{2 \sinh(\frac{\gamma^2}{4}\pi x)}. \quad (11)$$

(The factor  $\frac{1}{\sqrt{2}\eta(2i\tau)}$  is not present in [16] due to a different normalization of the Liouville theory on  $\mathcal{C}_\tau$ .) On the other hand, by (5) and (9),

$$\int_0^\infty Z(L, \ell) \ell^{ix} d\ell = \frac{3\sqrt{3}}{4} \frac{\sinh(\pi x)}{\sinh(\frac{4\pi x}{3}) + \frac{\sqrt{3}}{2}x} L^{ix-1}. \quad (12)$$

The surface corresponding to  $Z^{\text{t}}(L, \ell)$  can be analyzed in the probabilistic framework [23], as done in [14]. The counterpart of (12) is

$$\int_0^\infty Z^{\text{t}}(L, \ell) \ell^{ix} d\ell = \frac{3\sqrt{3}}{4} \frac{\sinh(\frac{\pi x}{3})}{\sinh(\frac{2\pi x}{3})} L^{ix-1}. \quad (13)$$

Since  $Z^{\text{nt}}(L, \ell) = Z(L, \ell) - Z^{\text{t}}(L, \ell)$ , combining (10)–(13), we arrive at

$$\begin{aligned} & \int_0^\infty p_B(e^{-2\pi\tau}, 1) \eta(2i\tau) e^{-\frac{2\pi x^2 \tau}{3}} d\tau \\ &= \frac{\sqrt{3}}{x} \left( \frac{\sinh(\frac{2}{3}\pi x) \sinh(\pi x)}{\sinh(\frac{4}{3}\pi x) + \frac{\sqrt{3}}{2}x} - \sinh(\frac{1}{3}\pi x) \right). \end{aligned}$$

This gives (2).

*Concluding remarks.*—The CFT aspect for percolation is a classical yet active topic [28]. The one-arm exponent and the polychromatic arm exponents have a CFT interpretation [29]. It would be highly desirable to find a CFT interpretation for the backbone exponent  $x_B$ . The expansion (2) is reminiscent of the closed channel expansion in boundary CFT, where  $\mathcal{S}$  can be thought of as the bulk spectrum. We can also expand in the open channel; see [14, Equation (1.4)]. In this expansion a logarithmic structure emerges. We thus suspect that there is an interesting logarithmic CFT that captures  $x_B$ .

The monochromatic  $k$ -arm exponent for  $k \geq 3$  lies strictly between the polychromatic  $k$ - and  $(k+1)$ -arm exponents [2]. Its precise value remains unknown. Unlike the backbone exponent, we have not found an effective conformal radius encoding that can be solved via the method in [13].

The methods for deriving  $x_B$  and  $p_B(r, R)$  are both quite general: they can be applied to any 2D lattice model whose scaling limit is described by a CLE, such as the random cluster model and the  $O(n)$  loop model. For example, in [5], we also derived the backbone exponent for the random cluster model, which corresponds to  $\text{CLE}_\kappa$  with  $\kappa \in (4, 8)$ . In [30], we derive the nested-path exponent defined in [31] for the random cluster model. We plan to investigate arm exponents of other models, such as the one-arm exponent of CLE percolation and

the Fuzzy Potts model [25, 32]. We also plan to derive the annulus partition function of various lattice models under conformal boundary conditions.

*Acknowledgements.*— P.N. is partially supported by a GRF grant from the Research Grants Council of the Hong Kong SAR (project CityU11318422). W.Q. and X.S. are supported by National Key R&D Program of China (No. 2023YFA1010700). Z.Z. is partially supported by NSF grant DMS-1953848. We thank B. Duplantier for helpful comments.

---

\* bpmnolin@cityu.edu.hk

† weiqian@cityu.edu.hk

‡ xinsun@bicmr.pku.edu.cn

§ zijie123@wharton.upenn.edu

- [1] S. R. Broadbent and J. M. Hammersley, *Proc. Cambridge Philos. Soc.* **53**, 629 (1957).
- [2] V. Beffara and P. Nolin, *Ann. Probab.* **39**, 1286 (2011).
- [3] M. P. M. den Nijs, *Journal of Physics A: Mathematical and General* **12**, 1857 (1979); H. Saleur and B. Duplantier, *Phys. Rev. Lett.* **58**, 2325 (1987); M. Aizenman, B. Duplantier, and A. Aharony, *Phys. Rev. Lett.* **83**, 1359 (1999); S. Smirnov and W. Werner, *Math. Res. Lett.* **8**, 729 (2001).
- [4] G. F. Lawler, O. Schramm, and W. Werner, *Electron. J. Probab.* **7**, no. 2, 13 (2002).
- [5] P. Nolin, W. Qian, X. Sun, and Z. Zhuang, (2023), [arXiv:2309.05050 \[math.PR\]](#).
- [6] P. Grassberger, *Physica A: Statistical Mechanics and its Applications* **262**, 251 (1999); Y. Deng, H. W. J. Blöte, and B. Nienhuis, *Phys. Rev. E* **69**, 026114 (2004); S. Fang, D. Ke, W. Zhong, and Y. Deng, *Phys. Rev. E* **105**, 044122 (2022).
- [7] O. Schramm, *Israel J. Math.* **118**, 221 (2000).
- [8] S. Smirnov, *C. R. Acad. Sci. Paris Sér. I Math.* **333**, 239 (2001).
- [9] B. Duplantier, *Phys. Rev. Lett.* **81**, 5489 (1998); later proved using SLE in G. F. Lawler, O. Schramm, and W. Werner, *Acta Math.* **187**, 275 (2001); *Acta Math.* **189**, 179 (2002).
- [10] V. G. Knizhnik, A. M. Polyakov, and A. B. Zamolodchikov, *Mod. Phys. Lett. A* **3**, 819 (1988).
- [11] B. Duplantier and S. Sheffield, *Invent. Math.* **185**, 333 (2011).
- [12] A. M. Polyakov, *Phys. Lett. B* **103**, 207 (1981).
- [13] M. Ang, N. Holden, and X. Sun, *Comm. Pure Appl. Math.* **77**, 2651 (2024).
- [14] X. Sun, S. Xu, and Z. Zhuang, (2024), [arXiv:2410.04767 \[math.PR\]](#).
- [15] J. Cardy, *J. Phys. A* **35**, L565 (2002); *J. Stat. Phys.* **125**, 1 (2006).
- [16] M. Ang, G. Remy, and X. Sun, (2022), [arXiv:2203.12398 \[math.PR\]](#).
- [17] F. Camia and C. M. Newman, *Comm. Math. Phys.* **268**, 1 (2006); S. Sheffield, *Duke Math. J.* **147**, 79 (2009).
- [18] O. Schramm, S. Sheffield, and D. B. Wilson, *Comm. Math. Phys.* **288**, 43 (2009).
- [19] G. Lawler, O. Schramm, and W. Werner, *J. Amer. Math. Soc.* **16**, 917 (2003).
- [20] see e.g. J. Ambjørn and Y. Watabiki, *Nuclear Physics B* **445**, 129 (1995); D. Boulatov and V. Kazakov, *Physics Letters B* **186**, 379 (1987); O. Angel and O. Schramm, *Comm. Math. Phys.* **241**, 191 (2003).
- [21] N. Holden and X. Sun, *Acta Math.* **230**, 93 (2023).
- [22] J. Bettinelli and G. Miermont, *Probab. Theory Related Fields* **167**, 555 (2017).
- [23] S. Sheffield, *Ann. Probab.* **44**, 3474 (2016); B. Duplantier, J. Miller, and S. Sheffield, *Astérisque*, viii+257 (2021).
- [24] G. Remy and T. Zhu, *Comm. Math. Phys.* **395**, 179 (2022).
- [25] J. Miller, S. Sheffield, and W. Werner, *Forum Math. Pi* **5**, e4, 102 (2017).
- [26] F. David, *Mod. Phys. Lett. A* **3**, 1651 (1988); J. Distler and H. Kawai, *Nucl. Phys. B* **321**, 509–527 (1989).
- [27] E. J. Martinec, (2003), [arXiv:hep-th/0305148](#).
- [28] B. Nienhuis, *J. Statist. Phys.* **34**, 731 (1984); P. Di Francesco, H. Saleur, and J. B. Zuber, *Nucl. Phys. B* **285**, 454 (1987); J. L. Cardy, *J. Phys. A* **25**, 201 (1992); R. Nivesvivat, S. Ribault, and J. L. Jacobsen, *SciPost Phys.* **17**, 029 (2024), [arXiv:2311.17558 \[hep-th\]](#).
- [29] Y. He, J. L. Jacobsen, and H. Saleur, *JHEP* **12**, 019 (2020), [arXiv:2005.07258 \[hep-th\]](#).
- [30] M. Ang, X. Sun, P. Yu, and Z. Zhuang, (2024), [arXiv:2401.15904 \[math.PR\]](#).
- [31] Y.-F. Song, X.-J. Tan, X.-H. Zhang, J. L. Jacobsen, B. Nienhuis, and Y. Deng, *J. Phys. A* **55**, Paper No. 204002, 11 (2022).
- [32] L. Köhler-Schindler and M. Lehmkuehler, (2022), [arXiv:2209.12529 \[math.PR\]](#).